Reactive Sulfur Species: Kinetics and Mechanism of the Oxidation of Cystine by Hypochlorous Acid to Give N,N‘-Dichlorocystine

ARTICLE *in* CHEMICAL RESEARCH IN TOXICOLOGY · JULY 2005

Impact Factor: 3.53 · DOI: 10.1021/tx050079r · Source: PubMed

2 AUTHORS, INCLUDING:

Péter Nagy
National Institute of Oncology
56 PUBLICATIONS **990** CITATIONS

Reactive Sulfur Species: Kinetics and Mechanism of the Oxidation of Cystine by Hypochlorous Acid to Give N,N′-Dichlorocystine

Péter Nagy and Michael T. Ashby*

Department of Chemistry and Biochemistry, University of Oklahoma, Norman, Oklahoma 73019

Received March 19, 2005

Cystine and HOCl (a neutrophil-derived oxidant) react to form an intermediate that has a half-life of ca. 5 min at pH 7.5. The intermediate subsequently decomposes to eventually yield a mixture of cystine, higher oxides of Cys, and other uncharacterized species. Spectral titrations, transitory ^{1}H NMR and UV−vis spectra, and the reaction properties of the intermediate are consistent with a formulation of N,N′-dichlorocystine {NDC = $[-SCH_2CH(NHCl)(CO_2H)]_2$}. The reaction of equimolar amounts of HOCl with cystine at pH 11.3 does not yield N-chlorocystine [NCC = $(^-O_2C)(H_3N^+)CHCH_2SSCH_2CH(NHCl)(CO_2H)$] but rather a 1:1 mixture of NDC and cystine. This result could be explained by two mechanisms: rapid disproportionation of NCC to produce NDC and cystine or a faster reaction of the second equivalent of HOCl with NCC than the first equivalent of HOCl reacts with cystine. The latter mechanism is favored because of our observation by NMR spectroscopy that NDC decomposes via a species that we have assigned as NCC. Thus, disproportionation of NCC is apparently a relatively slow process. The rates of reaction of cystine^0 = $[-SCH_2CH(NH_3^+)(CO_2^-)]_2°$, cystine^{1-} = $[(^-O_2C)(H_2N)CHCH_2SSCH_2CH(NH_3^+)(CO_2^-)]^-$, and cystine^{2-} = $[-SCH_2CH(NH_2)(CO_2^-)]_2^{2-}$ have been investigated, and it is clear that cystine^0 is unreactive, whereas cystine^{2-} is about four times more reactive than cystine^{1-}. Accordingly, the following mechanism is proposed (constants for 5 °C): $HOCl = H^+ + OCl^-$, pK_1 = 7.47; cystine^0 = cystine^{1-} + H^+, pK_2 = 8.15; cystine^{1-} = cystine^{2-} + H^+, pK_3 = 9.00; cystine^{1-} + HOCl → NCC^{1-} + H_2O, $k_4 = 4.3(2) \times 10^6$ M^{-1} s^{-1}; cystine^{2-} + HOCl → NCC^{2-} + H_2O, $k_5 = 1.6(2) \times 10^7$ M^{-1} s^{-1}; NCC^{1-} → NCC^{2-} + H^+, k_6 = fast; NCC^{2-} + HOCl → NDC^{2-} + H_2O, k_7 = fast. At physiologic pH, the k_4 pathway dominates. The generation of long-lived chloramine derivatives of cystine may have physiological consequences, since such compounds are known to react with nucleophiles via mechanisms that are also characteristic of HOCl, electrophilic transfer Cl^+.

Introduction

Diseases caused by atherosclerosis are the leading cause of morbidity and mortality in developed countries. The oxidative modification hypothesis of atherosclerosis envisages that low-density lipoprotein (LDL) oxidation contributes to atherogenesis (*1*). Buttressing this hypothesis are the observations that oxidized LDL supports foam cell formation in vitro, that lipids in human lesions are considerably oxidized, that there is evidence for the presence of oxidized LDL in vivo, that oxidized LDL has many potentially proatherogenic activities, and that several structurally unrelated antioxidants inhibit atherosclerosis in animal models (*1*). Perplexingly, despite the availability of abundant circumstantial data that indicate a causal role of oxidative stress in atherogenesis and the progression of the disease, dietary (*2*) and pharmaceutical (*3*) antioxidant strategies have exhibited poor performance in limiting atherosclerosis in humans. A recent review noted that current antioxidant strategies "presuppose a detailed knowledge of the relevant oxidants involved" when in fact relatively little information is available regarding the nature of these oxidants in a complex biological setting (*1*). Most of the antioxidants that have been investigated to date (e.g., probucol, vitamin E, and butylated hydroxyl toluene) have been chosen because they inhibit LDL oxidation in vitro by 1e-oxidants (e.g., radical species). Hence, there has been considerable interest in determining the relative reactivity of antioxidants toward 1e-oxidants (*5*). However, there is mounting anecdotal evidence that 2e-oxidants, such as the neutrophil-derived reactive oxygen species (ROS) hypochlorous acid (HOCl), may play significant roles in LDL damage (*4*). Both inorganic and organic reductants may be involved in reactions with HOCl in vivo. For example, we have recently proposed that thiocyanate (SCN^-) may limit the lifetime of HOCl in human blood plasma by its reaction with HOCl to produce hypothiocyanite ($OSCN^-$), a species that is not lethal to mammalian cells (*6*). Motivated by the possible causal relationship between LDL oxidation and atherosclerosis, Pattison and Davies have investigated the rates of reaction of HOCl with the components of proteins and lipids (*7*−*9*). It has been suggested that the relative rates of reaction of HOCl with protein components at physiological pH are Met > Cys ≫ cystine ∼ His ∼ α-amino > Trp > Lys ≫ Tyr ∼ Arg > backbone amides > Gln ∼ Asn (*7*). However, it is not clear for most of these reactions if long-lived reactive intermediates might be generated (secondary ROS), and in some cases, the products are not known. For cystine, it has been suggested that the disulfide bond, and not the amine groups, is the site of initial attack by HOCl (*7*). We report here the kinetics and mechanism of the reaction of cystine with HOCl, as

* To whom correspondence should be addressed. E-mail: MAshby@ou.edu.

10.1021/tx050079r CCC: $30.25
Published on Web 06/01/2005

well as transient spectra, which evidence that N,N′-dichlorocystine (NDC) is exclusively generated when modest ratios of cystine:HOCl are reacted, and that NDC exhibits a substantial lifetime at physiologic pH.

Materials and Methods

Materials. Water was doubly distilled in glass. L-Cystine, L-cysteine, L-cysteic acid monohydrate, L-cysteinesulfinic acid monohydrate, peracetic acid, deuterium chloride (35 wt %) solution in D_2O, $NaClO_4$, and K_3PO_4 were used as received from Sigma-Aldrich. $Na_3PO_4{\cdot}12H_2O$ was used as received from Mallinckrodt. Deuterium oxide (99.9%) was obtained from Cambridge Isotope Laboratories. The concentrations of stock solutions of OCl^- were determined iodometrically. The concentration of OCl^- in solutions that were prepared from the stock solution of commercial bleach was confirmed spectrophotometrically [$\epsilon(OCl^-)_{292nm} = 350\ M^{-1}\ cm^{-1}$].

pH/pD Measurements. pH measurements were made with an Orion ion Analyzer EA920 using a Ag/AgCl combination pH electrode. All pH measurements were corrected for the "Irving factor" of the working medium (*10*), and a temperature correction was applied. pD measurements in D_2O were made using the same pH electrode by adding 0.4 units to the measurement.

Synthesis of L-Cystine S-Monoxide. A literature procedure was followed with slight modification (*11*). Peracetic acid (8.5 mM, 32 wt % solution in dilute acetic acid) was added dropwise to a solution of L-cystine (1.0 g, 4.2 mmol) in H_2SO_4 (1 M, 10 mL) at 0 °C with stirring. After the mixture was stirred for 16 h at 0 °C, the pH was adjusted to 4 with cold pyridine. The product was precipitated with EtOH (50 mL) as a white solid, isolated by filtration, washed sequentially with EtOH (10 mL) and Et_2O (5 mL), and dried under vacuum. The crude product was recrystallized from ice-cold acetic acid upon addition of acetone. After isolation by filtration, the product was washed with MeOH (5 mL) and Et_2O (5 mL) and dried under vacuum at room temperature. ^1H NMR of the L-cystine S-monoxide showed some cystine impurity (ca. 10%). To evidence formation of the monoxide rather than the dioxide, the product was hydrolyzed at pH 11.3 to produce a 1:1 mixture of cystine and cysteine sulfinic acid ($CySO_2H$).

Stopped-Flow Studies. Kinetic measurements were made with a HI-TECH SF-61 DX2 stopped-flow spectrophotometer using a Xe arc lamp. Temperature control of the observation cell was maintained with a Lauda RC-20 circulator. The monochromatic kinetic traces were fitted with HI-TECH KinetAsyst 3.14 software (Hi-Tech, United Kingdom). Time-resolved spectra were fitted using SPECFIT 3.0.36 global analysis software (Spectrum Associates, Chapel Hill, NC). All data points represent the average of at least nine shots. The cystine and H^+ dependencies of the rate law were determined under pseudo-first-order conditions at $\lambda = 250$ and 300 nm. Time-resolved UV−vis spectra were assembled from individual kinetic traces that were measured under second-order conditions in the $\lambda = 230-300$ nm range in 5 nm increments.

NMR Studies. ^1H NMR spectra were recorded with a Varian XL-300 spectrometer at 298.0 (±0.5) K. Deuterated buffers were prepared from D_2O solutions of anhydrous K_3PO_4 by adding DCl. The chemical shifts (ppm) were referenced to sodium 3-(trimethylsilyl)-1-propane-sulfonate ($\delta = 0.015$ ppm). Turbulent mixing of reagents was necessary to ensure homogeneity of reaction mixtures in the time frame of chemical reaction, and this was achieved for the NMR studies by employing a hand mixer comprised of two Hamilton syringes and a T-mixer. Failure to quickly mix solutions of HOCl and cystine produced different, unreproducible results. For NDC, ^1H NMR (300 MHz, pH 7.5): δ 3.83 (dd, 2H, $^3J_{\alpha\text{-}\beta} = 5$ Hz, $^3J_{\alpha\text{-}\beta'} = 7$ Hz, H_α), 3.17 (dd, 2H, $^3J_{\beta\text{-}\beta'} = 14$ Hz, H_β), 3.03 (dd, 2H, H_β'). ^1H NMR (300 MHz, pH 11.3): δ 3.80 (dd, 2H, $^3J_{\alpha\text{-}\beta} = 5$ Hz, $^3J_{\alpha\text{-}\beta'} = 7$ Hz, H_α), 3.17 (dd, 2H, $^3J_{\beta\text{-}\beta'} = 14$ Hz, H_β), 3.02 (dd, 2H, H_β'). For NCC, ^1H NMR (300 MHz, pH 7.5): δ 4.11 (dd, 1H, $^3J_{\alpha\text{-}\beta} = 4$ Hz, $^3J_{\alpha\text{-}\beta'} = 8$ Hz, $H_2NC\mathbf{H}CH_2S$), 3.82 (dd, 1H, $^3J_{\alpha\text{-}\beta} = 5$ Hz, $^3J_{\alpha\text{-}\beta'} = 7$ Hz, $ClHNC\mathbf{H}CH_2S$), 3.39 (dd, 1H, $^3J_{\beta\text{-}\beta'} = 15$ Hz, $H_2NCHC\mathbf{H}_2S$), 3.21 (dd, 1H, $^3J_{\beta\text{-}\beta'} = 14$ Hz, $ClHNCHC\mathbf{H}_2S$), 3.16 (dd, 1H, $H_2NCHC\mathbf{H}_2S$), 3.06 (dd, 1H, $ClHNCHC\mathbf{H}_2S$). For cystine, ^1H NMR (300 MHz, pH 7.5): δ 4.18 (dd, 2H, $^3J_{\alpha\text{-}\beta} = 4$ Hz, $^3J_{\alpha\text{-}\beta'} = 8$ Hz, H_α), 3.44 (dd, 2H, $^3J_{\beta\text{-}\beta'} = 15$ Hz, H_β), 3.26 (dd, 2H, H_β'). ^1H NMR (300 MHz, pH 11.3): δ 3.59 (dd, 2H, $^3J_{\alpha\text{-}\beta} = 5$ Hz,, $^3J_{\alpha\text{-}\beta'} = 8$ Hz, H_α), 3.12 (dd, 2H, $^3J_{\beta\text{-}\beta'} = 14$ Hz, H_β), 2.91 (dd, 2H, H_β').

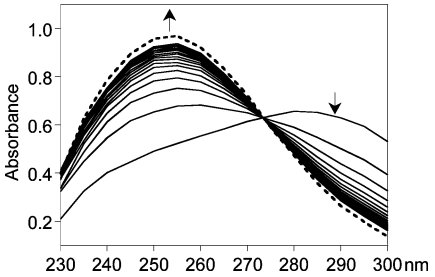

Figure 1. Time-resolved UV−visible spectra illustrating the consumption of OCl^- at 290 nm and the appearance of NDC at 255 nm: $[HOCl]_0^T = 1.8$ mM, phosphate buffer = 0.1 M, $[cystine]_0 = 1.0$ mM, pH = 11.3, $I = 0.45$ M ($NaCl + Na_2HPO_4 + Na_3PO_4$), and $T = 293$ K. These spectra were assembled from monochromatic kinetic traces that were spaced 5 nm apart. Note the isosbestic point. The dashed line was recorded at $t = 10$ s when the reaction was close to completion.

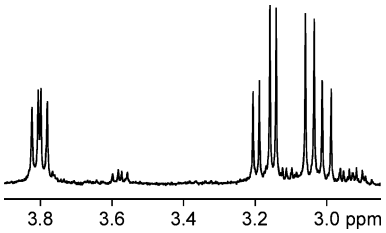

Figure 2. ^1H NMR spectrum of NDC at $T = 293$ K. The resonances at 3.02 and 3.17 ppm are assigned to the H_β protons, and the dd at 3.80 ppm is assigned to the H_α proton of NDC in pD 11.3 D_2O (referenced to DSS, the smaller peaks at ca. 2.93 ppm). The H_α resonances of cystine are beginning to appear at ca. 3.58 ppm and elsewhere. Note that the H_α resonance of cystine is very sensitive to pH, appearing at 3.58 at pH 11.3 but at 4.14 at pH 7.5 (Figure 3).

UV/vis Spectroscopy. Electronic spectra were measured using a HP 8452A diode array spectrophotometer or the monochromator of the HI-TECH SF-61 DX2 stopped-flow instrument with a Xe arc lamp.

Results

Figure 1 illustrates time-resolved UV−vis spectra for the reaction of cystine with HOCl/OCl^- at pH 11.3 and the consumption of OCl^- ($\lambda_{max} = 292$ nm) and formation of a initial product with $\lambda_{max} = 255$ nm and $\epsilon = 1150\ M^{-1}\ cm^{-1}$ (assuming a single molecular product). The initial product was further characterized by ^1H NMR spectroscopy (Figure 2). Similar ^1H NMR spectra were obtained for the initial product at pH 7.5, and the time-resolved ^1H NMR spectra of Figure 3 evidence the lifetime of the initial product that is formed after reacting cystine and HOCl/OCl^- near physiologic pH, as well as the subsequent formation of a second intermediate during the decomposition of the initial product. We note that the ^1H NMR spectrum of the second intermediate was not as clear at pH 11.3 due to the overlap of spectra and its more rapid decomposition. However, if cystine and HOCl/OCl^- are reacted at pH 11.3 and the pH is subsequently adjusted to 7.5, the same transient spectra for both the initial product and the second intermediate are observed

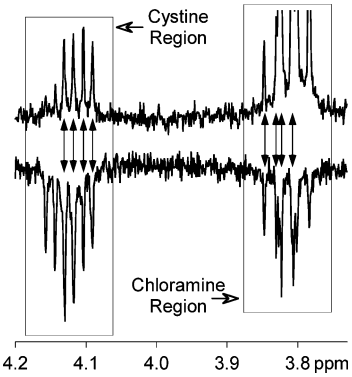

Figure 3. Time-resolved ^{1}H NMR spectra in the region of the H_α proton resonance of cystine (4.14 ppm) and NDC (3.80 ppm, off scale) after 5.5 (top) and 17 (bottom) min [flipped spectrum illustrating transient resonances that are assigned to NCC, two doublet of doublets (3.82 and 4.11 ppm) indicated by double arrows: $[HOCl]_0^T = 5.0$ mM, $[cystine]_0 = 2.5$ mM, and $T = 293$ K]. In addition to the transient resonances of NCC in the inverted spectrum, a resonance for cystine (4.14 ppm), another decomposition product of NDC, is also observed. The sample was prepared at pH 7.5 (225 mM phosphate) using a hand mixer (see Materials and Methods).

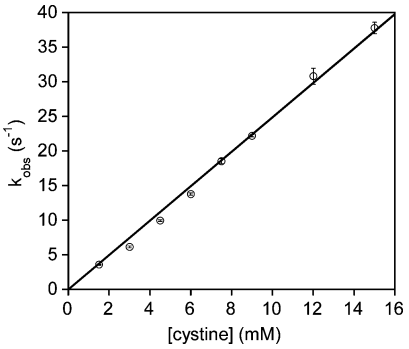

Figure 4. Cystine dependency of the rate law under pseudo-first-order conditions: $[HOCl]_0^T = 0.15$ mM, phosphate buffer = 0.1 M, [cystine] = 1.5−15 mM, pH = 11.3, $I = 1$ M [$NaClO_4$ + Na_2HPO_4 + Na_3PO_4 + Na_2(cystine)], and $T = 293$ K. Kinetic traces were evaluated at 300 nm.

as when the reaction is performed at pH 7.5. The stoichiometry of the reaction was investigated by ^{1}H NMR spectroscopy. Addition of two molar equivalents of HOCl/OCl^- to cystine produced one molar equivalent of the initial product (Figure 2). Addition of one molar equivalent of HOCl/OCl^- to cystine produced one-half molar equivalent of the initial product and one-half molar equivalent of unreacted cystine (data not shown). A similar stoichiometry is indicated when UV−visible spectrophotometry is used to follow the reaction (data not shown).

The kinetics of the reaction of cystine and HOCl/OCl^- were investigated at pH 11.3. Under pseudo-first-order conditions (excess cystine), the reaction rate is first-order with respect to the total concentration of HOCl ($[HOCl]^T$ = [HOCl] + [OCl^-]) and first-order with respect to cystine ($[cystine]_0^T$ = [$cystine^0$] + [$cystine^{1-}$] + [$cystine^{2-}$]) (Figure 4). The reaction kinetics are inversely dependent on the [OH^-] (Figure 5). The reaction rates of HOCl/OCl^- with cystine near neutral pH are too fast to follow by stopped-flow at 20 °C. However, the reaction can be followed at 5 °C for all [H^+] (Figure 6).

Discussion

It has been previously suggested that the disulfide moiety of cystine is targeted by HOCl/OCl^- (*7*). However,

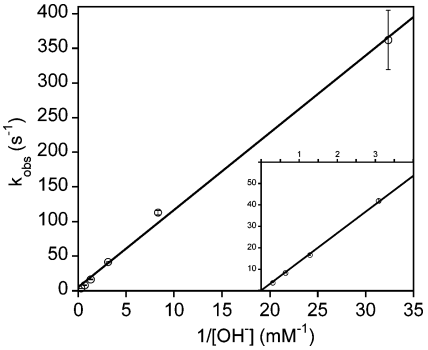

Figure 5. Hydroxide ion dependency of the rate law under pseudo-first-order conditions: $[HOCl]_0^T = 0.15$ mM, phosphate buffer = 0.1 M, [cystine] = 1.5 mM, pH = 9.28−11.3, $I = 1$ M [$NaClO_4$ + Na_2HPO_4 + Na_3PO_4 + Na_2(cystine)], and $T = 293$ K. Kinetic traces were evaluated at 300 nm.

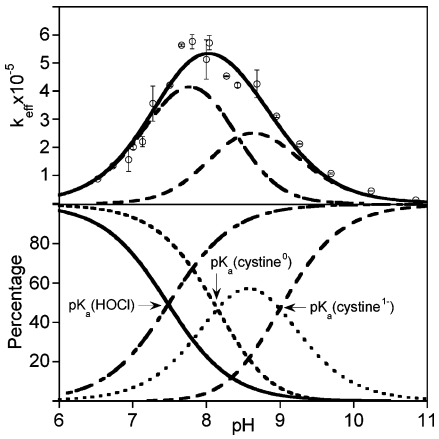

Figure 6. (Top) Computed k_{eff} for the k_4 pathway (dot−dashed), k_5 pathway (dashed), and combined k_4 and k_5 pathways (solid) at 5 °C. The observed k_{eff} (open circles) with standard deviations (as error bars) is also plotted. (Bottom) Computed speciation of HOCl (solid), OCl^- (dot−dashed), $cystine^0$ (short dashed), $cystine^{1-}$ (dotted), and $cystine^{2-}$ (long dashed) at 5 °C. The parameters that were employed to develop this figure were as follows: $K_1 = 3.39 \times 10^{-8}$ M^{-1}, $K_2 = 7.08 \times 10^{-9}$ M, $K_3 = 1.00 \times 10^{-9}$ M, $k_4 = 4.3 \times 10^6$ M^{-1} s^{-1}, and $k_5 = 1.6 \times 10^7$ M^{-1} s^{-1}. The pK_a values of HOCl, $cystine^0$, and $cystine^{1-}$ are indicated.

Scheme 1. Stoichiometry of the Reaction of Cystine with OCl^- at pH 11.3 and the Reaction of the Product with Cys (NMR Quantified Species Are in Bold)

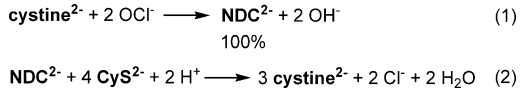

the electronic spectrum of the product (Figure 1, λ_{max} = 255 nm and $\epsilon = 1150$ M^{-1} cm^{-1}) is consistent with the formation of a chloramine. Aliphatic chloramines typically exhibit $\lambda_{max} \approx 245-260$ nm and $\epsilon \approx 300-420$ M^{-1} s^{-1} (*12*). The molar absorptivity of the product in Figure 1 is consistent with the formation of one chloramine moiety per equivalent of HOCl/OCl^-. The addition of two molar equivalents of HOCl/OCl^- produces a quantitative yield of NDC (Scheme 1, reaction 1). The stoichiometry observed in the NMR experiments and the symmetry of the ^{1}H NMR spectra are consistent with the formation of NDC. To rule out the possibility that the first product is the symmetrical cystine S,S′-dioxide, an unstable species that is expected to rearrange to cystine S,S-dioxide, the thiosulfinate ester (*13*), we subjected cystine S-monoxide, the thiosulfenate ester, to HOCl under

Scheme 2. Proposed Mechanism, Equilibrium, and Rate Constants (at 5 °C) and Rate Law for the Reaction of Cystine and HOCl for Pseudo-First-Order Conditions (Excess Cystine)

$$HOCl \rightleftharpoons H^+ + OCl^- \qquad K_1 = 10^{-7.47}\ M$$

$$cystine^0 \rightleftharpoons H^+ + cystine^{1-} \qquad K_2 = 10^{-8.15}\ M$$

$$cystine^{1-} \rightleftharpoons H^+ + cystine^{2-} \qquad K_3 = 10^{-9.00}\ M$$

$$cystine^{1-} + HOCl \longrightarrow NCC^{1-} + H_2O \qquad k_4 = 4.3\times10^6\ M^{-1}s^{-1}$$

$$cystine^{2-} + HOCl \longrightarrow NCC^{2-} + H_2O \qquad k_5 = 1.6\times10^7\ M^{-1}s^{-1}$$

$$NCC^{1-} \longrightarrow H^+ + NCC^{2-} \qquad k_6 = fast$$

$$NCC^{2-} + HOCl \longrightarrow NDC^{2-} + H_2O \qquad k_7 = fast$$

$$[HOCl]_0^T = [HOCl] + [OCl^-]$$

$$[cystine]_0^T = [cystine^0] + [cystine^{1-}] + [cystine^{2-}]$$

$$\frac{d[NCC]}{dt} = \frac{K_2(k_4[H^+]^2 + K_3k_5[H^+])[cystine]_0^T}{(K_1+[H^+])([H^+]^2 + K_2[H^+] + K_2K_3)}[HOCl]^T$$

similar reaction conditions. The spectrum of the symmetrical first product of Figure 2 was not observed; instead, the result was an unusually complicated spectrum that was consistent with the production of a large number of products. Furthermore, the first product that we observed in the reaction of HOCl/OCl^- and cystine (NDC) reacts with four molar equivalents of Cys to produce three molar equivalents of cystine (Scheme 1, reaction 2), a reaction that is consistent with its formulation as NDC.

Given our characterization of the first cystine-derived product of the reaction of cystine and HOCl/OCl^- as NDC, we interpret the observed kinetics according to the reaction mechanism and rate law of Scheme 2. The mechanism of Scheme 2 is consistent with the observed 2:1 HOCl/OCl^-:cystine stoichiometry as well as the observed first-order dependency of the concentrations of HOCl/OCl^- and cystine (Figure 4). Figure 5 illustrates an inverse relationship between [OH^-] (i.e., a first-order dependency on [H^+]), which suggests that HOCl is the reacting oxidant. The intercept of zero in Figure 5 (inset) demonstrates that OCl^- does not exhibit a measurable rate of reaction with cystine. The rates of reaction of HOCl with nucleophiles are typically 10^3−10^5 faster than OCl^- (*14*−*16*).

While it was possible to measure the kinetics of the reaction of HOCl/OCl^- with cystine at room temperature (20 °C) under very basic conditions, the reaction became too fast for such measurements near neutral pH. However, it proved possible to measure the rate between pH 6 and pH 11 at 5 °C (Figure 6). The reaction kinetics exhibit an inflection point with a maximum rate at about pH 8, which is indicative of a competitive acid−base equilibrium. The rate decreases above pH 8, which is consistent with reaction of HOCl and not OCl^-, since the pK_a of HOCl is 7.47 at 5 °C and $I = 1$ M. Our estimated pK_a value of HOCl at 5 °C is based upon previously measured values between 15 and 50 °C (*17*). The observed decrease in rate below pH 8 suggests that the amines, and not the ammonium moieties of cystine, are responsible for reactivity. We estimate the two pK_a values of the amines of cystine to be 8.15 and 9.00 at 5 °C based upon previously measured values at 25 and 36 °C (*18*).

While the analysis of the kinetics is thus far straightforward, two questions remain. Given the characterization of the product by ^{1}H NMR as NDC (a measurement that was made within 3 min of turbulent mixing of the reagents), one unresolved issue is the relative rates of production of N-chlorocystine (NCC) vs NDC. Given the lack of any spectral evidence for biphasic kinetics or observation of a different transient spectrum that might be assigned to NCC for the stoichiometry of 1:10 to 1:100 HOCl/OCl^-:cystine (the UV−vis and ^{1}H NMR spectra that resulted at pH 11.3 for the 1:10 ratio was consistent with a ca. 20:1 mixture of cystine and NDC), we believe that the reaction of the second equivalent of HOCl with NCC (Scheme 2, k_7) is much faster than the first reaction that produces NCC (Scheme 2, k_4 and k_5). However, these observations might be misleading if NCC undergoes rapid disproportionation to yield NDC and cystine. In addition to the fact that previously measured rates for disproportionation of chloramines are substantially slower than the observed formation of NDC by UV−vis and ^{1}H NMR (*19*, *20*), we have evidence that the disproportionation of NDC is slow. The transient ^{1}H NMR spectra that are observed for the decomposition of NDC at pH 7.5 (Figure 3) reveal the decomposition of NDC via an unsymmetrical species that has resonances at $\delta = 3.82$ and $\delta = 4.11$ ppm, very near the chemical shift of cystine and NDC, respectively. We have assigned this spectrum to NCC. The transient spectrum is observed to disappear with the formation of the spectrum of a mixture of cystine and cystic acid (the sulfonate of Cys). Accordingly, we believe that the formation of NDC is fast with respect to the reaction that produces NCC at modest ratios of cystine:HOCl.

A second question that remains unanswered is whether $cystine^{1-}$ and $cystine^{2-}$ exhibit similar reactivities. This is an important issue because the k_4 pathway is expected to dominate at physiologic pH. Figure 6 affords some insight. If only $cystine^{2-}$ were reactive, we would expect the maximum rate to be observed at about pH 8.6 (based upon on our accurate measurement of k_5 at high pH and our estimates of the relevant equilibrium constants). If $cystine^{1-}$ were the only cystine-derived reactant, we would expect a maximum rate to be observed at pH 7.8 for similar reasons. Given the expectation that $cystine^{1-}$ should not be more reactive than $cystine^{2-}$, the observed maximum rate at about pH 8.0 suggests that both mechanisms are operative. Furthermore, the magnitudes of the observed rate and the width-at-half-height of the k_{eff} vs pH (Figure 6, top) cannot be explained by the k_4 or the k_5 pathway alone. Using [H^+], k_4 and k_5 as variables in the equation of Scheme 2, we subjected the experimental data of Figure 6 to nonlinear least-squares analysis. That analysis yielded the rate constants $k_4 = 4.3(2) \times 10^6\ M^{-1}\ s^{-1}$ and $k_5 = 1.6(2) \times 10^7\ M^{-1}\ s^{-1}$ at 5 °C. These rate constants are consistent with values for k_4 and k_5 that were determined at the peripheries of Scheme 2, low pH and high pH, where the respective k_4 and k_5 pathways would dominate. Furthermore, the relative magnitudes of the rate constants, about 1:4, are consistent with the expectation that the dianion $cystine^{2-}$ should be a better nucleophile. However, despite the smaller rate constant for the reaction of $cystine^{1-}$, the k_4 pathway yields faster maximum rates because the pK_a of $cystine^0$ is better matched with the pK_a of HOCl as compared with the pK_a of $cystine^{1-}$.

To our knowledge, this is the first report of an absolute rate constant for the reaction of HOCl with cystine. Winterbourn et al. have previously estimated the rate constant for the reaction of cystine with HOCl/OCl^- by measuring the yield of a competitive trap for HOCl (monochlorodimedone) (*21*). Pattison and Davies noted that this earlier study did not distinguish between the reaction of HOCl with the N or S groups of cystine, and they attempted to clarify this issue by measuring a rate constant for the reaction of HOCl/OCl^- with 3,3′-dithiopropionic acid (1.6×10^5 M^{-1} s^{-1} at pH 7.4 and 22 °C), which they have estimated to be the rate constant for "cystine" (*7*). Because their rate constant for 3,3′-dithiopropionic acid was comparable to the previous estimate for the rate constant for reaction of HOCl/OCl^- with cystine (ca. 10^5 M^{-1} s^{-1}), Pattison and Davies concluded that HOCl reacts with the S−S moiety of cystine (*7*). The present study demonstrates that the amine groups are in fact the sites of chlorination. Remarkably, the effective second-order rate constant that we have measured (3.8×10^5 M^{-1} s^{-1} at pH 7.4 and 5 °C) is very close to the value of 1.6×10^5 M^{-1} s^{-1} that was measured by Pattison and Davies for a disulfide bond when corrected for the difference in temperatures (*7*). Why then does cystine preferentially react to form chloramines? It is conceivable that the disulfide bond of 3,3′-dithiopropionic acid is more reactive than the disulfide bond of cystine, since the former compound is dianionic, whereas cystine^0 would predominate at neutral pH. Once deprotonated, the amine group of cystine^{1-} is apparently more reactive than the disulfide bond. We note that neither the intermediate nor the final products of the reaction of 3,3′-dithiopropionic acid and HOCl were characterized in the aforementioned previous study (*7*).

The longevity of NCC and NDC is perhaps the most significant observation of this study. The transient ^{1}H NMR spectra of Figure 3 illustrate that NCC and NDC retain their ability to oxidize, as expected for chloramines (*12*). In the absence of sacrificial reductants, NCC and NDC eventually oxidize their own sulfur centers, presumably via sulfenyl derivatives that are themselves reactive sulfur species (RSS) (*22*). Accordingly, it is conceivable that NCC and NDC play a role as secondary reactive oxidants in vivo (*23*). Indeed, such oxidants could prove more insidious, since it is well-recognized that more powerful oxidants, such as HOCl, are indiscriminant. Reactions such as the one described herein foretell that a complex mixture of ROS is likely to develop in the milieu of species that begins with primary ROS like HOCl and end with thermodynamically stable oxidized moieties that are frequently employed as biomarkers for oxidative stress (like chlorinated aromatic residues) (*24*). It is plausible that many of these terminal electron donors actually react with secondary ROS such as chloramines. We conclude by noting that the aforementioned possible role of NCC and NDC as secondary ROS and RSS applies to free cystine only. Once incorporated into a protein, the N centers of cystine are expected to be less reactive, and the SS bond would be expected to be the site of attack by HOCl.

Acknowledgment. This work was supported by the Oklahoma Center for the Advancement of Science and Technology (HR02-019).

Supporting Information Available: Derivation of the rate law, representative kinetic traces and fits, tables of kinetic data, and the Mathematica files that were used in the simulations. This material is available free of charge via the Internet at http://pubs.acs.org.

References

(1) Stocker, R., and Keaney, J. F., Jr. (2004) Role of oxidative modifications in atherosclerosis. *Physiol. Rev. 84*, 1381−1478.
(2) Schwenke, D. C. (1998) Antioxidants and atherogenesis. *J. Nutr. Biochem. 9*, 424−445.
(3) Aviram, M. (2000) Review of human studies on oxidative damage and antioxidant protection related to cardiovascular diseases. *Free Radical Res. 33*, S85−S97.
(4) Heinecke, J. W. (2003) Oxidative stress: New approaches to diagnosis and prognosis in atherosclerosis. *Am. J. Cardiol. 91*, 12A−16A.
(5) Buettner, G. R. (1993) The pecking order of free radicals and antioxidants: Lipid peroxidation, a-tocopherol, and ascorbate. *Arch. Biochem. Biophys. 300*, 535−543.
(6) Ashby, M. T., Carlson, A. C., and Scott, M. J. (2004) Redox buffering of hypochlorous acid by thiocyanate in physiologic fluids. *J. Am. Chem. Soc. 126*, 15976−15977.
(7) Pattison, D. I., and Davies, M. J. (2001) Absolute rate constants for the reaction of hypochlorous acid with protein side chains and peptide bonds. *Chem. Res. Toxicol. 14*, 1453−1464.
(8) Pattison, D. I., Hawkins, C. L., and Davies, M. J. (2003) Hypochlorous acid-mediated oxidation of lipid components and antioxidants present in low-density lipoproteins: Absolute rate constants, product analysis, and computational modeling. *Chem. Res. Toxicol. 16*, 439−449.
(9) Hawkins, C. L., Pattison, D. I., and Davies, M. J. (2003) Hypochlorite-induced oxidation of amino acids, peptides and proteins. *Amino Acids 25*, 259−274.
(10) Irving, H. M. N. H., Miles, M. G., and Pettit, L. D. (1967) A study of some problems in determining the stoichiometric proton dissociation constants of complexes by potentiometric titrations using a glass electrode. *Anal. Chim. Acta 38*, 475−488.
(11) Walti, M., and Hope, D. B. (1971) Synthesis of the isomers of the mono- and di-hydroxy-analogues of cystine and comparison with metabolites excreted in the urine. *J. Chem. Soc. Perkin Trans. 1 12*, 2326−2328.
(12) Kovacic, P., Lowery, M. K., and Field, K. W. (1970) Chemistry of N-bromamines and N-chloramines. *Chem. Rev. 70*, 639−665.
(13) Lacombe, S. M. (1999) Oxysulfur compounds derived from disulfides: stability and reactivity. *Rev. Heteroat. Chem. 21*, 1−41.
(14) Gerritsen, C. M., and Margerum, D. W. (1990) Nonmetal redox kinetics: Hypochlorite and hypochlorous acid reactions with cyanide. *Inorg. Chem. 29*, 2757−2762.
(15) Fogelman, K. D., Walker, D. M., and Margerum, D. W. (1989) Nonmetal redox kinetics: Hypochlorite and hypochlorous acid reactions with sulfite. *Inorg. Chem. 28*, 986−993.
(16) Kumar, K., and Margerum, D. W. (1987) Kinetics and mechanism of general-acid-assisted oxidation of bromide by hypochlorite and hypochlorous acid. *Inorg. Chem. 26*, 2706−2711.
(17) Adam, L. C., Fabian, I., Suzuki, K., and Gordon, G. (1992) Hypochlorous acid decomposition in the pH 5−8 region. *Inorg. Chem. 31*, 3534−3541.
(18) Martell, A. E., and Smith, R. M. (1989) *Crit. Stab. Constants 6* (2nd Suppl.).
(19) Gray, E. T., Jr., Margerum, D. W., and Huffman, R. P. (1978) Chloramine equilibriums and the kinetics of disproportionation in aqueous solution, *ACS Symp. Ser. 82*, 264−277.
(20) Snyder, M. P., and Margerum, D. W. (1982) Kinetics of chlorine transfer from chloramine to amines, amino acids, and peptides. *Inorg. Chem. 21*, 2545−2550.
(21) Winterbourn, C. C. (1985) Comparative reactivities of various biological compounds with myeloperoxidase-hydrogen peroxide-chloride, and similarity of the oxidant to hypochlorite. *Biochim. Biophys. Acta 840*, 204−210.
(22) Ashby, M. T., and Aneetha, H. (2004) Reactive sulfur species: Aqueous chemistry of sulfenyl thiocyanates. *J. Am. Chem. Soc. 126*, 10216−10217.
(23) Winterbourn, C. C. (1995) Free radical toxicology and antioxidant defense. *Clin. Exp. Pharmacol. Physiol. 22*, 877−880.
(24) Armstrong, D., Ed. (2002) *Oxidative Stress Biomarkers and Antioxidant Protocols*, *Methods in Molecular Biology*, Vol. 186, Humana Press, Totowa, NJ.

TX050079R